Mathematical Problems in Engineering
Volume 6, pp. 267–304
Reprints available directly from the publisher
Photocopying permitted by license only

Robustness with Respect to Disturbance Model Uncertainty: Theory and Application to Autopilot Performance Analysis

DANIEL E. DAVISON[†], PIERRE T. KABAMBA
and SEMYON M. MEERKOV*

Department of Electrical Engineering and Computer Science,
University of Michigan, 1301 Beal Avenue, Ann Arbor, MI 48109-2122, USA

(Received 10 September 1999)

Dedicated to the 60th birthday of Professor Robert E. Skelton

This paper deals with the notion of disturbance model uncertainty. The disturbance is modeled as the output of a first-order filter which is driven by white noise and whose bandwidth and gain are uncertain. An analytical expression for the steady-state output variance as a function of the uncertain bandwidth and gain is derived, and several properties of this variance function are analyzed. Two notions, those of *disturbance bandwidth margin* and *disturbance gain margin*, are also introduced. These tools are then applied to the analysis of a simple altitude-hold autopilot system in the presence of turbulence where the turbulence scale is treated as an uncertain parameter. It is shown that the autopilot, which is satisfactory for nominal turbulence scale, may be inadequate when the uncertainty is taken into account. Moreover, it is proven that, in order to obtain a design that provides robust performance in the face of turbulence scale uncertainty, it is necessary to substantially increase the controller bandwidth, even if one is willing to sacrifice the autopilot's holding ability and stability robustness.

Keywords: Aircraft control; Disturbance rejection; Model uncertainty; Robustness analysis

* Corresponding author. Tel.: (734) 763-6349. Fax: (734) 763-8041.
E-mail: smm@eecs.umich.edu.
[†] Present address: Cambridge University Engineering Department, Trumpington Street, Cambridge, CB2 1PZ, UK.

NOMENCLATURE (Excluding the Appendix)

A, B, C, D	state-space realization matrices
c	a constant used in Theorem 4.3
$C(s)$	generic controller transfer function
$C_i(s)$	particular controller transfer function ($i = 1, 2$)
$C_{\text{open}}(s)$	open-loop controller transfer function
d	disturbance signal (turbulence velocity)
$F(s)$	disturbance filter transfer function
$\bar{F}(s)$	$P_2(s)F(s)H(s)$,
g	acceleration due to gravity
$G(s)$	closed-loop transfer function from d to y
$\bar{G}(s)$	closed-loop transfer function from d to $\bar{y}$ ($\bar{G}(s) = G(s)H(s)$)
h	airplane altitude
$H(s)$	filter used to generate $\bar{y}$
K	disturbance gain
K^*	nominal value of K
L	turbulence scale
L_0	observability Grammian of (C, A)
$M_{\max}(\omega)$	upper bound on $\lvert S(j\omega)\rvert$
$P_i(s)$	plant transfer function ($i = 1, 2$)
r	command reference signal (desired altitude deviation)
$S(s)$	sensitivity function ($S(s) = 1/[1 + P_1(s)P_2(s)C(s)]$)
u	control signal (elevator deviation)
U	aircraft airspeed
$V(G)$	V-transform of G
w	Gaussian white noise with unit power spectral density
W	a weighting function used in Theorems 4.2 and 4.3
y	plant output signal (altitude deviation)
z	non-minimum-phase zero in the plant model
$\bar{y}$	filtered output signal (vertical acceleration)
α_i	a constant used in Theorem 4.2 ($i = 1, 2$)
γ	generic variance threshold
δ_e	elevator deflection
σ_w	turbulence intensity
ω	angular frequency
ω_b	disturbance bandwidth ($2U/L$)

ω_b^*	nominal value of ω_b
Ω	closed-loop system bandwidth
$\|\|S\|\|_\infty$	infinity norm of S (supremum of $\|S(j\omega)\|$)

FOREWORD

National Transportation Safety Board preliminary report #IAD99FA052 cites the following incident involving a passenger jetliner's encounter with turbulence [1]: On July 8, 1999 the Boeing 737 was cruising at 8800 m [29000 ft] over the Atlantic Ocean. Visual meteorological conditions prevailed, and, according to the first officer, "there were no visual cues to an adverse ride." The aircraft was flying through smooth air, when, suddenly, it encountered turbulence, resulting in seventy-two injured persons (one serious) and minor airplane damage. The aircraft was consequently diverted to make an emergency landing.

One interpretation of this incident is that the aircraft encountered turbulence of a different nature than the turbulence model used in the autopilot design and evaluation. In other words, the root cause of this incident may be considered to be a relative lack of robustness with respect to *disturbance model uncertainty*. The work described in this paper is devoted to analysis of the robustness of controllers (in particular, autopilots) with respect to uncertainty in the disturbance model.

1 INTRODUCTION

One of the objectives of feedback control is to attenuate disturbances. Typically, it is assumed that the disturbance belongs to a given class of signals (e.g., stochastic processes with given power spectral density), and a controller is designed to accommodate such disturbances in a desirable manner. The question of what happens if the actual disturbance is outside of the assumed class is usually ignored, even though there is often considerable uncertainty as to whether or not the disturbance is, in fact, in the class. For example, it is common to model

continuous wind turbulence [2–5], road roughness [6–10], and water waves [11–13] as stationary stochastic processes with *fixed* power spectral density (PSD), in spite of the fact that, in each case, the actual disturbance statistics are uncertain, and, moreover, they vary in both time and space. The goal of this paper is to introduce tools to analyze performance robustness with respect to uncertainty in disturbance bandwidth and power, and to apply these tools to an altitude-hold autopilot in the presence of uncertain turbulence.

The single-input single-output system under consideration is shown in Fig. 1. The transfer function C and transfer functions P_1 and P_2 comprise the controller and plant, respectively. Dividing the plant into two components allows us to model both input and output disturbances in a unified manner. The disturbance is assumed to be the output of the filter

$$F(s) = K\frac{\sqrt{2\omega_b}}{s+\omega_b}, \tag{1}$$

where ω_b and K are positive constants whose values may be uncertain. This structure of F was chosen since the parameters ω_b and K correspond to physically meaningful quantities: the disturbance bandwidth is ω_b and the disturbance root-mean-square (rms) value is K. Moreover, it is shown below that filter (1) corresponds to a model of turbulence cited in the literature [14]. Extensions of some of the results to more general disturbance filters are published elsewhere [15,16].

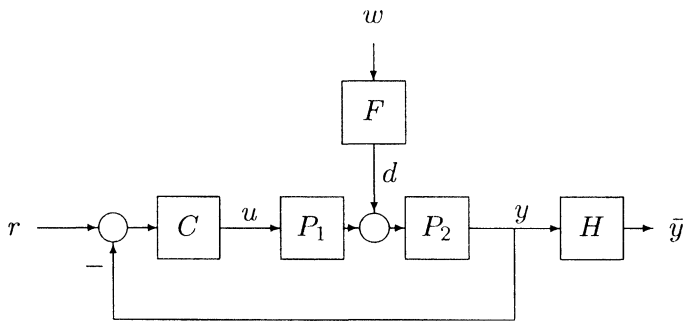

FIGURE 1 System model.

Robustness with respect to uncertainty in ω_b and K will be evaluated by computing, as a function of ω_b and K, the variance (i.e., rms squared) of several signals in Fig. 1; for presentation purposes, the focus will be on the variance of the filtered output signal, $\bar{y}$. Variance is a useful performance measure in many applications. For example, there is a relationship between passenger comfort and the variance of vertical acceleration in airplanes [2,5] and automobiles [7,9,17,18]. As another example, variance is closely related to the notions of *probability of exceedence* and *residence time*, concepts that are important in several fields of study, including aiming control (telescope pointing, missile terminal guidance, robot arm pointing, etc.) [19–21], aircraft gust load analysis [22,23], and ship stabilization in waves [24]. As a consequence of the practical importance of variance as a performance measure, the control literature uses variance extensively (e.g., in covariance control [25]).

For simplicity, sensor noise is assumed to be negligible over the bandwidth of the controller, and the reference signal is assumed to vary sufficiently slowly that the only contribution to the signal variance is the disturbance, d. It is also assumed that the disturbance is not measurable. Finally, to ensure the existence of an internally-stabilizing controller, it is assumed that H is stable and that there are no unstable pole-zero cancellations in forming the product P_1P_2.

As stated earlier, it is uncommon to explicitly account for uncertainty in the disturbance model. However, there are several relevant threads of research in the systems community. For example, Poor and Looze recognize that disturbance model uncertainty is a significant issue when they deal with the problem of *state estimation* under process and measurement noise [26]. They study cases where the PSD of one of the noise sources is uncertain and where the other is white noise with known PSD. In the scalar-state case, they also mention the *spectral band noise model* (originally used in [27], and subsequently in [28], in the context of noncausal signal estimation in the presence of uncertain noise) in which the PSD of the fixed-power noise signal is assumed to lie between known lower and upper bounds. The approach of their paper is to optimize the worst-case mean-square error by forming a minimax optimization problem. Earlier papers of a similar nature include [29] and [30]. Poor and Looze also contributed to [31], where the LQG problem is considered in the face of uncertain process

and measurement noise. Both noise sources, however, are assumed to be white (i.e., there is assumed to be no *frequency-dependent* uncertainty in the PSDs). Again, a minimax optimization approach is taken. More recently, Chen and Dong consider the LQG problem subject to both plant parametric uncertainty and uncertain noise PSD; however, the noise is again assumed to be white with uncertainty only in the magnitude of the PSD [32]. Other papers that treat the LQG problem with white noise and uncertainty in the noise covariance include [33] and [34].

The second thread is that of Gusev, who considers problems where a portion of the correlation function of the disturbance is assumed to belong to a prespecified set [35–37]. For both control and filtering problems, he develops minimax design procedures, although the tools used are distinctly different from the previously mentioned papers.

The third strategy for treating estimation problems with uncertain plant state-space matrices and uncertain noise statistics is the use of *bounding filters* [38–40]. The idea is to design for a spectrum that bounds the possible noise spectra. As discussed in [30], this simple approach can be useful, but it also can lead to conservative designs and, moreover, it is not applicable if the noise spectra cannot be bounded. A bounding approach is also used in a recent paper dealing with the LQG problem in the face of uncertain disturbances [41].

It is possible to rearrange Fig. 1 into a so-called *generalized plant*; having done so, the uncertainty in F is transformed into uncertainty in the generalized plant. Since the general $\mathcal{H}_2$ problem can be posed as an LQG problem (with cross-weights in the cost function), LQG theory dealing with parametric plant uncertainty is also relevant to this paper. Many researchers have tackled this subject area, although it seems that few papers include cross-weights in the performance index, so most results are not directly applicable to the problem at hand. Nevertheless, a brief review is appropriate: Grimble treats uncertain plant parameters in the LQG problem as *random variables* [42]. The author describes a method of choosing the LQG weights to improve stability robustness. A random variable approach is also taken by Ray, where an active suspension system is considered using statistical (Monte Carlo) analysis [43]. McDowell and Basar also treat uncertain plant parameters as random variables, but the authors consider performance in addition to stability [44]. The approach of their work

is to minimize the expected cost. Alternative approaches to the random variable method include a minimax approach to plant parameter uncertainty [45] and the approach of Bernstein and Greeley, in which the authors handle plant parameter uncertainty in the LQG problem by introducing artificial multiplicative noise sources at the uncertain parameters [46]. Yet another approach is to use the *parameter robust LQG* method, where parameter variations are treated by introducing artificial internal feedback loops [47,48].

In spite of this significant body of literature, simple tools for analysis of the robustness of control systems with respect to disturbance model parameter uncertainty are lacking. This paper is written to contribute to this end, and is organized as follows. In Section 2 the main analysis tool, the V-transform, is defined; V-transforms give convenient expressions for signal variance, explicitly as a function of K and ω_b. In Section 3 two robustness margins, the disturbance gain and bandwidth margins, are defined in terms of V-transforms to quantify how much uncertainty in ω_b and K can be tolerated before performance becomes unacceptable. These concepts are then applied in Section 4 to an autopilot system to show that a seemingly good controller design lacks robustness with respect to uncertainty in turbulence scale. In the same section, the issue of *robustness performance limitations* is discussed, and it is shown that the robustness can be made satisfactory only by increasing the closed-loop bandwidth significantly. Conclusions are given in Section 5, and proofs are collected in the Appendix.

2 THE V-TRANSFORM

Temporarily assume that K in (1) is unity. Then the variance of $\bar{y}$, as a function of $\bar{G}$ and ω_b, is defined by what is referred to here as a V-transform:

$$V(\bar{G})(\omega_b) \triangleq \|\bar{G}F\|_2^2 = \frac{1}{\pi}\int_0^\infty |\bar{G}(j\omega)|^2 \frac{2\omega_b}{\omega_b^2 + \omega^2}\, d\omega, \tag{2}$$

where the V stands for "variance". The word "transform" is used since $V(\bar{G})$ transforms $\bar{G}$, a function of s, into a function of ω_b. For general

K, the variance of $\bar{y}$ is $K^2 V(\bar{G})(\omega_b) = V(K\bar{G})(\omega_b)$. The following theorem describes several properties of $V(\bar{G})$ as a function of ω_b:

THEOREM 2.1 *Let $\bar{G}$ be a stable proper transfer function with state-space realization*

$$\bar{G}(s) = \left[\begin{array}{c|c} A & B \\ \hline C & D \end{array}\right](s) \triangleq D + C(sI - A)^{-1}B.$$

Then

- *$V(\bar{G})$ is a rational function of ω_b that is proper and has "state-space realization"*

$$V(\bar{G})(\omega_b) = \left[\begin{array}{c|c} A & B \\ \hline 2(B^{\mathrm{T}}L_o + DC) & D^2 \end{array}\right](\omega_b), \tag{3}$$

  where L_o is the observability Grammian of (C, A), i.e., the unique solution to

$$A^{\mathrm{T}}L_o + L_o A + C^{\mathrm{T}}C = 0. \tag{4}$$

- *$V(\bar{G})$ is an analytic, nonnegative, and bounded function of ω_b.*
- $V(\bar{G})(0) = \bar{G}(0)^2$.
- $\lim_{\omega_b \to \infty} V(\bar{G})(\omega_b) = D^2$.

The first statement in the theorem is used to conveniently compute V-transforms. The Lyapunov equation (4) is linear in L_o, so it can be solved to any prespecified accuracy in a finite number of operations. Note that the variance of any signal in Fig. 1, not just $\bar{y}$, can be written in terms of V-transforms (e.g., the variance of u is $K^2 V(GC)$). Also note that V-transforms need not be monotonic functions of ω_b, and, therefore, it's not possible to determine the "worst-case" ω_b (the one that yields maximum variance) without computing the corresponding V-transform. A deeper study of V-transforms, including their mathematical properties and an example showing that V-transforms provide information that is not easily obtained from Bode plots, is available in [49].

3 DISTURBANCE ROBUSTNESS MARGINS

Let $\gamma > 0$ denote the threshold of the variance of $\bar{y}$ that determines acceptable performance. Assume that

$$V(K^*\bar{G})(\omega_b^*) < \gamma,$$

that is, nominal performance is achieved. It's natural to quantify how much K and ω_b can vary from their nominal values before (if ever) performance becomes unacceptable. Define the *disturbance gain margin* (DGM) to be the largest increase in K that can be tolerated until performance becomes unacceptable:

$$\text{DGM} \triangleq \left(\frac{\gamma}{V(K^*\bar{G})(\omega_b^*)}\right)^{1/2}.$$

In general, two margins are needed to account for uncertainty in ω_b since $V(\bar{G})$ need not be a monotonic function of ω_b. However, for the autopilot example in the next section, it is sufficient to define a single margin, the *disturbance bandwidth margin* (DBM), as the largest *increase* in ω_b that can be tolerated until performance becomes unacceptable:

$$\text{DBM} \triangleq \sup\left\{\frac{\bar{\omega}_b}{\omega_b^*}: \bar{\omega}_b \geq \omega_b^* \text{ and } \forall \omega_b \in [\omega_b^*, \bar{\omega}_b], V(K^*\bar{G})(\omega_b) \leq \gamma\right\}.$$

(For convenience define the supremum of an unbounded set of positive real numbers to be infinity. Also, if nominal performance is not achieved, define DBM to be zero.)

The concepts of disturbance gain margin and disturbance bandwidth margin appear to be new. Both margins are easily determined from a plot of the relevant V-transform. For example, Fig. 2 shows $V(G)$ where $G(s) = s/(s+1)$; assuming $K^* = 1$, $\omega_b^* = 1$, and $\gamma = 0.8$, one obtains

$$\text{DBM} = \frac{4.0}{1.0} = 4.0 \quad \text{and} \quad \text{DGM} = \left(\frac{0.8}{0.5}\right)^{1/2} = 1.26.$$

That is, the system can tolerate an increase in disturbance bandwidth up to a factor of 4.0, or an increase in disturbance gain up to a factor

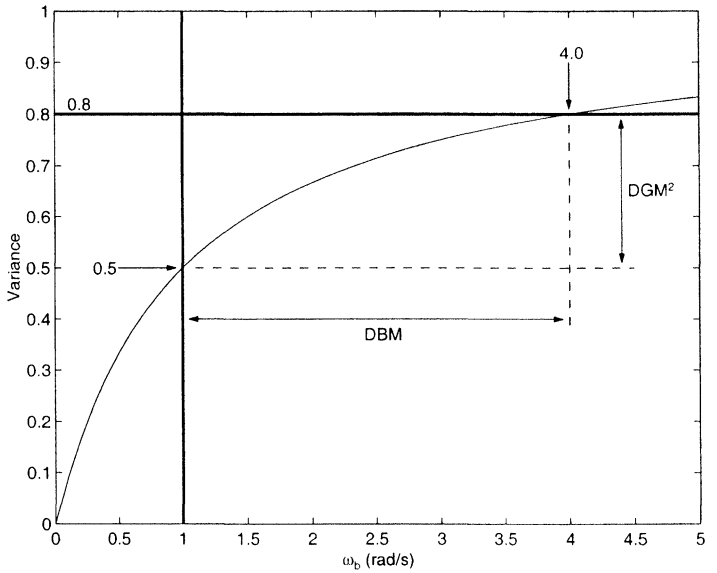

FIGURE 2 V-transform of $G(s)=s/(s+1)$ illustrating the computation of DBM and DGM.

of 1.26, before the variance exceeds the threshold. Note that the definitions of DGM and DBM, as with V-transforms, apply equally well to signals in Fig. 1 other than $\bar{y}$.

4 APPLICATION TO AN ALTITUDE-HOLD AUTOPILOT

4.1 Scenario

In this section, we consider the effect of turbulence uncertainty on the performance of an altitude-hold autopilot. The plane is an F-89 jet aircraft cruising at 6100 m [20000 ft] at Mach 0.638 (200 m/s [660 ft/s]); this plane has been selected for analysis for no special reason except that its dynamical model is readily available [23]. The autopilot that will be considered uses the elevator (with deflection δ_e) to control the altitude. For simplicity, throttle is not used as a second actuator, and it is assumed that the aircraft is flying in a vertical plane. For the turbulence analysis, it will be assumed that the aircraft is flying in "clear air" turbulence.

The performance of the autopilot will be quantified by standard measures such as command tracking response, stability margins, and bandwidth. The effect of turbulence will be evaluated using four measures:

- *Altitude-holding ability:* The deviation of the aircraft from its nominal altitude will be quantified by rms(h). To ensure that the aircraft does not deviate more than 60 m [200 ft], a 20 m [67 ft] threshold is set on rms(h).
- *Elevator angle variation:* To avoid excessive elevator motion, a 0.5 deg threshold is set on rms(δ_e).
- *Elevator rate variation:* To ensure that the elevator is not commanded to move too quickly, a 5 deg/s threshold is placed on rms($\dot{\delta}_e$).
- *Passenger comfort:* There is experimental evidence that passenger comfort is related to rms($\ddot{h}$), as the data in Table I, taken from [5], indicates. Assume that under clear air turbulence conditions the autopilot should result in, at most, "moderate" discomfort. According to Table I, the rms vertical acceleration should correspondingly not exceed 0.15g.

For future use, the threshold information is summarized in the fourth row of Table II. The thresholds were chosen based on a combination of intuition and values known to be reasonable for other aircraft; the particular values do not necessarily correspond to real data for the aircraft and flight conditions being considered here.

The plane and turbulence models in this scenario fit into the scheme of Fig. 1 where u is the deviation of δ_e from its nominal value, y is the deviation of h from 6100 m, $\bar{y}$ is the acceleration $\ddot{h}$, d is the turbulence

TABLE I Relationship between airplane travel comfort and rms vertical acceleration

Qualitative description of turbulence	*rms vertical acceleration (in g's)*
Negligible	0.05
Slight	0.10
Moderate	0.10–0.15
Moderately heavy	0.20–0.30
Severe	0.30–0.60
Extreme	0.60

TABLE II Comparison of the rms value of several signals for controllers C_1, C_2, and C_{open}. The turbulence model parameters are at their nominal values

	$rms(\ddot{h})$(*in g's*)	$rms(h)$ (*in* m)	$rms(u)$ (*in* deg)	$rms(\dot{u})$(*in* deg/s)
$C_1(s)$	0.137	0.69	0.060	0.155
$C_2(s)$	0.102	0.69	0.263	6.790
$C_{\text{open}}(s)$	0.115	∞	0.000	0.000
Threshold	0.150	20.0	0.500	5.000

velocity, and r is the desired deviation in altitude from 6100 m. In the following subsections, the plant and disturbance models are given, a proportional-derivative (PD) controller is presented, the controller is analyzed with respect to uncertainty in the turbulence bandwidth (and found to be inadequate), it is shown that a large increase in the closed-loop bandwidth is necessary to improve the robustness, and a modified PD controller is suggested.

4.2 Airplane Model

Using the information in [23], the transfer functions from u (in rad) to y (in m) and d (in m/s) to y (in m) can be computed to be

$$\frac{y(s)}{u(s)} = \frac{21.275(s+19.8114)(s-17.0301)(s+0.0064)}{s(s^2+4.2087s+18.2546)(s^2+0.0090s+0.0040)},$$

$$\frac{y(s)}{d(s)} = \frac{-1.43(s+3.8443)(s^2+0.0055s+0.0131)}{s(s^2+4.2087s+18.2546)(s^2+0.0090s+0.0040)}.$$

Thus, a suitable choice for the plant transfer functions in Fig. 1 is

$$P_1(s) = \frac{21.275(s+19.8114)(s-17.0301)(s+0.0064)}{-1.43(s+3.8443)(s^2+0.0055s+0.0131)},$$

$$P_2(s) = \frac{-1.43(s+3.8443)(s^2+0.0055s+0.0131)}{s(s^2+4.2087s+18.2546)(s^2+0.0090s+0.0040)}.$$

Filter $H(s)$ is set to s^2 since $y=h$ and $\bar{y}=\ddot{h}$. Note that the plant is non-minimum-phase; denote the non-minimum-phase zero at $s=17.0301$ by z. The plant is also unstable; the instability mandates the use of feedback control to obtain acceptable altitude-hold characteristics. In the analysis to follow, uncertainty in the plant model is accounted for

only when stability margins are discussed; it is assumed that the plant model is accurate when the robustness to turbulence model uncertainty is evaluated.

4.3 Turbulence Model

Under the flight conditions considered here it is reasonable to assume that the turbulence is homogeneous and isotropic [4]. A widely used model of the vertical component of the wind velocity is that of a stationary stochastic process with the Von Kármán PSD [4]:

$$\sigma_w^2 \frac{L}{U} \frac{1 + \frac{8}{3}(1.339L\omega/U)^2}{[1 + (1.339L\omega/U)^2]^{11/6}}.$$

In this formula, σ_w^2 is the power (i.e., variance) of the wind (in $(\text{m/s})^2$), L is the so-called turbulence scale (in m) and U is the true airspeed of the aircraft (200 m/s). Because it is not possible to generate a signal with the Von Kármán spectrum by passing white noise through a linear time-invariant (LTI) finite-dimensional filter, it is common to approximate the Von Kármán spectrum by the rational Dryden spectrum [4] or the even simpler rational spectrum [14]

$$\sigma_w^2 \frac{L}{U} \frac{4}{4 + (L\omega/U)^2}. \tag{5}$$

Spectrum (5) is used in this paper. A signal with this spectrum is generated by filtering white noise through the disturbance filter (1) with

$$K = \sigma_w \quad \text{and} \quad \omega_b = \frac{2U}{L}. \tag{6}$$

Note that L affects ω_b only, and ω_b is inversely proportional to L.

The values of σ_w and L vary greatly depending on the altitude and the nature and severity of the turbulence. At the assumed altitude, Ref. [4] recommends setting σ_w to 1.46 m/s [4.8 ft/s] for clear air turbulence, so $K^* = 1.46$ m/s. For simplicity, K will be assumed to be fixed at K^* for the remainder of the paper.[‡] The choice of L is less

[‡] Uncertainty in K is easily handled since the variance of all signals is proportional to K^2; thus, the largest admissable K is the worst-case value.

clear: For the Von Kármán model it is recommended that L be set to 762 m [2500 ft], but for the Dryden model a value of 533 m [1750 ft] is standard [4]. Since spectrum (5) is closer to the Dryden model than the Von Kármán model, the nominal L value is chosen to be 533 m. The corresponding nominal wind bandwidth is, via (6), $\omega_b^* = 0.754$ rad/s. Uncertainty arises in ω_b because of the underlying uncertainty in L. As an estimate of the degree of uncertainty, consider that values of L as small as 150 m [490 ft] and as large as 1500 m [4900 ft] have been proposed in the literature for the Von Kármán model [2]; the corresponding values of ω_b are 2.7 rad/s and 0.27 rad/s respectively. Therefore, we will demand satisfactory performance (as measured by rms($\ddot{h}$), rms(h), rms(u) and rms($\dot{u}$)) for all $\omega_b \in [0.27, 2.7]$ rad/s.

4.4 PD Controller and Nominal Controller Performance

As suggested in [23], a simple but effective autopilot design is to feed back h and $\dot{h}$ to the elevator. The PD-like controller

$$C_1(s) = -0.0023 \frac{s + 0.15}{0.1s + 1} \tag{7}$$

was found to yield good command tracking response, good stability margins (gain margin = 3.4 = 10.6 dB, phase margin = 63 deg, $\|S\|_\infty =$ 1.50 = 3.5 dB), and reasonable close-loop bandwidth (gain crossover frequency = 1.0 rad/s and effectively no control effort[§] is used above 7.0 rad/s). Plots of the command tracking ability (in the absence of turbulence), loop-gain Bode plot, and magnitude of the sensitivity function are shown as solid curves in Figs. 3–5. (The other curves in the figures are explained below.) The rms($\ddot{h}$), rms(h), rms(u), and rms($\dot{u}$) values for *nominal* ω_b and K, tabulated in the first row of Table II, are seen to be less than the corresponding thresholds, so nominal turbulence behavior is deemed acceptable. The table also shows that the open-loop control C_{open} (i.e., any controller which does not use feedback) has satisfactory nominal rms($\ddot{h}$), rms(u), and rms($\dot{u}$), but, as mentioned previously, the open-loop controller has no altitude-holding ability (i.e., rms(h) = ∞), and is therefore not useful. (The data

[§] This notion of bandwidth is defined more precisely later.

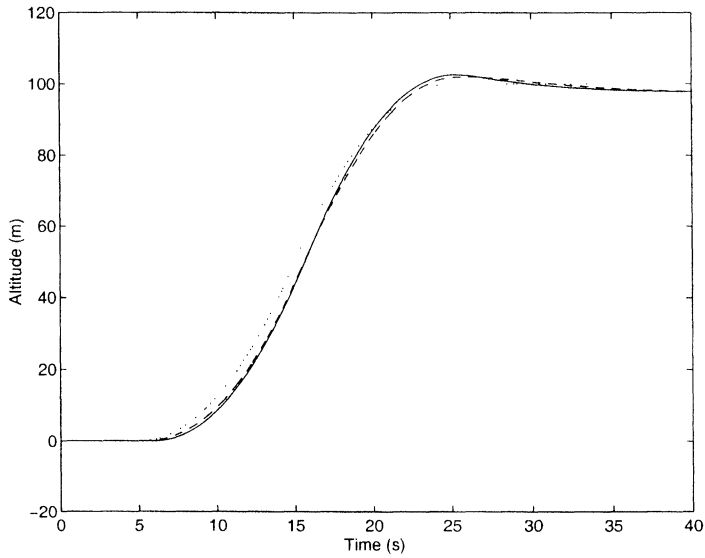

FIGURE 3 Command tracking for controller (7) (solid) and controller (13) (dashed). The dotted curve is the commanded trajectory.

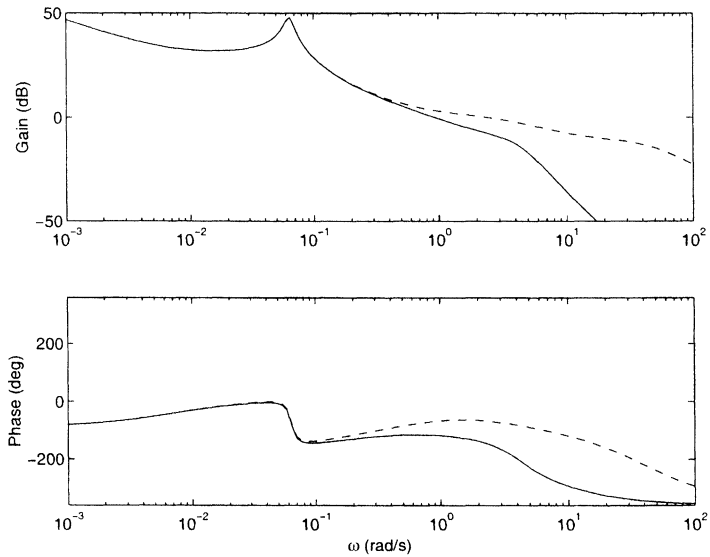

FIGURE 4 Loop-gain Bode plot for controller (7) (solid) and controller (13) (dashed)

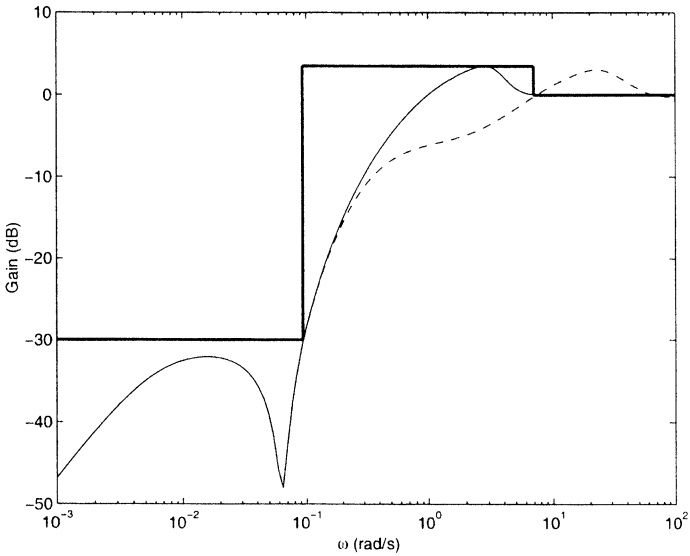

FIGURE 5 Sensitivity magnitude plot for controller (7) (solid) and controller (13) (dashed). The thick solid lines represent the performance boundary used in the derivation of PLC-3, drawn for $\Omega = 7$ rad/s.

in the first three rows of Table II is obtained from Figs. 6–9, presented in the next subsection.)

4.5 Robustness Analysis

In this section the robustness of C_1 with respect to changes in ω_b is evaluated. Plots of rms($\ddot{h}$), rms(h), rms(u), and rms($\dot{u}$), for nominal K, are shown in Figs. 6–9 as solid curves. The four curves were generated by computing the square roots of $V(K^*\bar{G})$, $V(K^*G)$, $V(K^*GC_1)$, and $V(K^* \cdot s \cdot GC_1)$, respectively, all via Theorem 2.1. In each plot, a thick vertical line is drawn at the nominal ω_b (0.754 rad/s), a thick horizontal line is drawn at the corresponding performance threshold (see the fourth row of Table II), and two dotted vertical lines mark the boundary of the interval [0.27, 2.7]. The other curves in the figures are explained below.

Figures 7–9 reveal that, for ω_b in the range [0.27, 2.7], the rms values of h, u, and $\dot{u}$ are acceptable. (The corresponding DBM values are

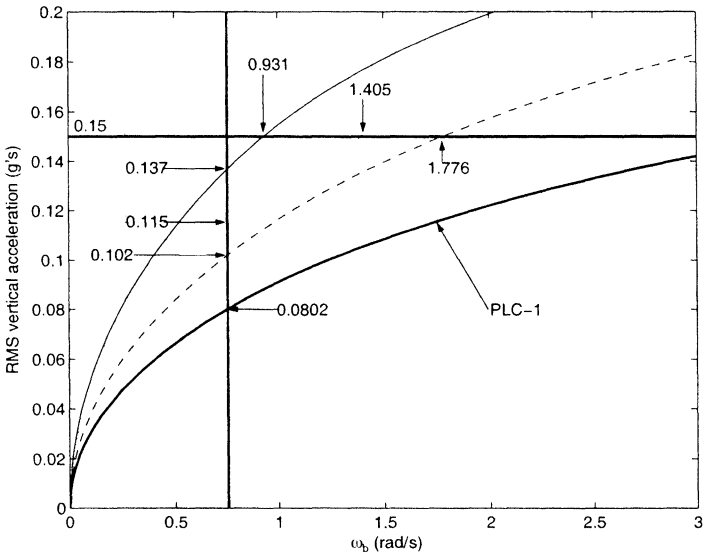

FIGURE 6 Plot of rms($\ddot{h}$) for controller (7) (solid), for controller (13) (dashed), and for open-loop control (dotted). Also shown in thick solid lines are the performance limitation curve PLC-1, the performance threshold, and the nominal ω_b value. The two dotted vertical lines mark the ω_b interval of interest.

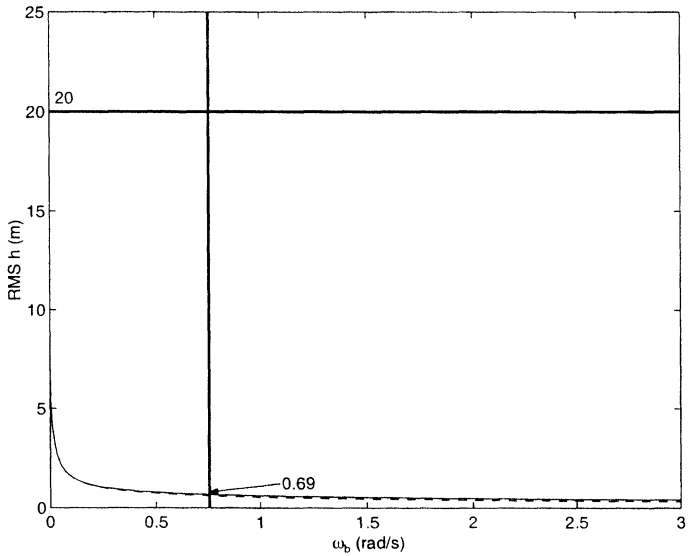

FIGURE 7 Plot of rms(h) for controller (7) (solid) and for controller (13) (dashed). Also shown is the performance threshold and the nominal ω_b value. The two dotted vertical lines mark the ω_b interval of interest.

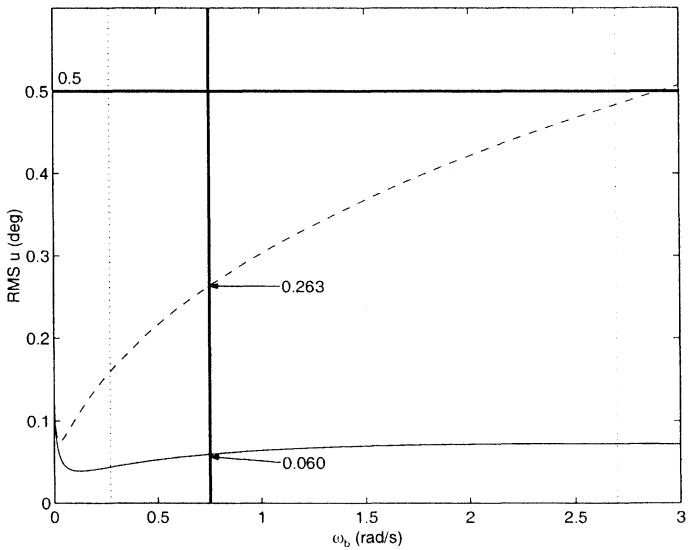

FIGURE 8 Plot of rms(u) for controller (7) (solid) and for controller (13) (dashed). Also shown is the performance threshold and the nominal ω_b value. The two dotted vertical lines mark the ω_b interval of interest.

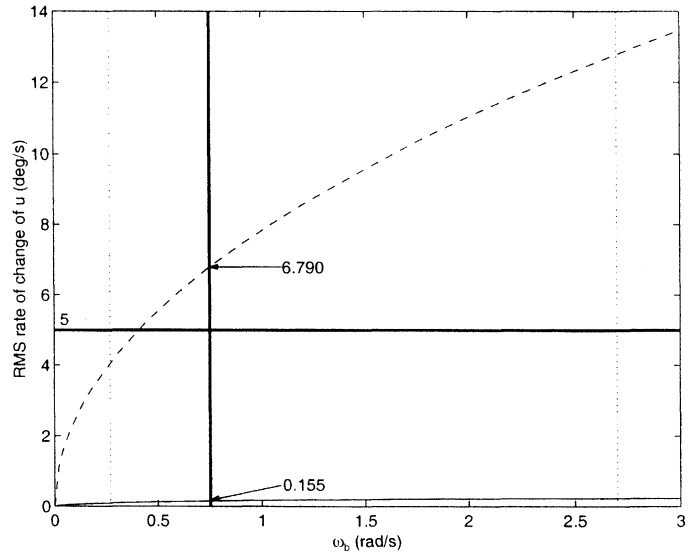

FIGURE 9 Plot of rms($\dot{u}$) for controller (7) (solid) and for controller (13) (dashed). Also shown is the performance threshold and the nominal ω_b value. The two dotted vertical lines mark the ω_b interval of interest.

TABLE III Comparison of the robustness of controllers C_1, C_2, and C_{open} with respect to uncertainty in ω_b. The figures in the last row are based on the requirement that ω_b values as large as 2.7 be accommodated, i.e., the required DBM is $2.7/0.754 = 3.58$

	DBM for $\ddot{h}$	*DBM for* (h)	*DBM for* (u)	*DBM for* $\dot{u}$
C_1	1.23	∞	∞	∞
C_2	2.36	∞	3.85	0.00
C_{open}	1.86	0.00	∞	∞
Minimum acceptable value	3.58	3.58	3.58	3.58

listed in the first row of Table III. They were obtained by inspecting the figures on a wider range of ω_b than shown.) In contrast, it is apparent from Fig. 6 that, when uncertainty in ω_b is accounted for, the rms value of $\ddot{h}$ is not acceptable. Indeed, from Fig. 6, the performance robustness margins for $\ddot{h}$ can be computed to be

$$\text{DBM} = \frac{0.931}{\omega_b^*} = 1.23 \quad \text{and} \quad \text{DGM} = \frac{0.15}{0.137} = 1.09.$$

The low value of DGM is not of concern since it is a measure of robustness with respect to uncertainty in K, and K is assumed to be fixed here. A concerning lack of robustness, however, is reflected in the relatively low value of DBM: If ω_b is only 23% larger than the nominal ω_b^* (corresponding to ω_b greater than 0.931 rad/s or L less than 432 m [1418 ft]), then the variance of $\ddot{h}$ will be unacceptable. Since values of ω_b as large as 2.70 rad/s can be expected, an increase in the robustness with respect to uncertainty in ω_b is needed. Note that the open-loop control, although superior to C_1 in terms of the rms of $\ddot{h}$, also has inadequate DBM (see the dotted curve in Fig. 6 and the third and fourth rows in Table III).

4.6 Improving the Robustness of the PD Controller

At this point, it has been shown that, although C_1 has acceptable nominal performance, the robustness of rms$(\ddot{h})$ with respect to ω_b is inadequate, that is, DBM is too low. It is reasonable to try to modify C_1 to improve DBM for $\ddot{h}$; however, it is desirable to maintain the low bandwidth, good stability margins, and good altitude-hold

characteristics of C_1. This leads to the issue of *robustness performance limitations*, that is, determination if there exist fundamental limitations on how much the robustness can be improved. This question is addressed in this subsection by computing *performance limitation curves*, that is, lower bounds on the achievable V-transforms. Since the only signal with inadequate robustness properties is $\ddot{h}$, we compute performance limitation curves (PLC's) only for $V(K^*\bar{G})$. Three different PLC's, each more sophisticated than the previous one, are considered, then a controller whose robustness is superior to that of C_1 is suggested. An in-depth discussion on the derivation computation, and interpretation of the PLC formulae is available in [15].

4.6.1 PLC-1: No Constraints Other than Stability

In order to determine if *any* internally-stabilizing LTI controller can achieve the desired DBM for $\ddot{h}$, initially relax all considerations of bandwidth, stability robustness, and holding ability. Then the following PLC is obtained:

THEOREM 4.1 *For every internally-stabilizing controller, the variance of* $\ddot{h}$ *satisfies, for every* $\omega_b > 0$,

$$\text{var}(\ddot{h}) = V(K\bar{G})(\omega_b) > \frac{\beta\omega_b K^2}{(z+\omega_b)^2}, \tag{8}$$

where β *is a constant that depends only on the plant data and* z. *The bound is tight, in the sense that, for any specific* $\omega_b > 0$, *a controller can be found so that* $V(K\bar{G})(\omega_b)$ *is arbitrarily close to achieving equality in* (8) *at that value of* ω_b.

For the airplane system, constant β is 121.83. The lower bound in (8) (with appropriate unit conversion) is shown in Fig. 6, marked PLC-1 (for "performance limitation curve 1"). The bound intersects the performance threshold ($0.15g$) at $\omega_b = 3.52$ rad/s, and its value at nominal ω_b is $0.0802g$. This performance limitation curve therefore places an upper bound on the robustness margins for $\ddot{h}$:

$$\text{DBM} \leq \frac{3.52}{\omega_b^*} = 4.67 \quad \text{and} \quad \text{DGM} \leq \frac{0.15}{0.0802} = 1.87. \tag{9}$$

That is, no internally-stabilizing LTI controller can achieve a DBM larger than 4.67, or, equivalently, no internally-stabilizing LTI controller can satisfy the rms threshold for $\ddot{h}$ if L is less than 114 m [375 ft]. (Similarly, no internally-stabilizing controller can achieve a DGM value larger than 1.87, or, equivalently, satisfy the rms threshold if the turbulence intensity is greater than 2.73 m/s [8.96 ft/s].) Fortunately, 4.67 is larger than the required DBM of 3.58 (see Table III).

The Controller that attains variance arbitrarily close to the lower bound in (8) was computed using the construction given in the proof of the theorem. By adjusting the value of ω_b used for the controller design, DBM for $\ddot{h}$ can be made arbitrarily close to the theoretical limit of 4.67. Unfortunately, regardless of which ω_b is used in the minimum-variance controller design, the resulting controller uses essentially infinite bandwidth, has infinitesimal stability margins, exhibits extremely poor altitude-hold properties, and uses unrealistic control effort. In fact, controllers that exactly achieve the bound in (8) yield a closed-loop system with a pole at the origin. Moreover, the minimum-variance controllers are all of high order. Clearly such controllers are impractical. Nevertheless, PLC-1 shows that at least there exists a LTI controller with the desired DBM.

Remark 4.1 The fact that the variance bound in Theorem 4.1 is nonzero is due strictly to the non-minimum-phase zero in the plant. In general, it can be shown that if P_1P_2 in Fig. 1 is non-minimum-phase, then the variance of $\bar{y}$ cannot be made arbitrarily small; in contrast, in the minimum-phase case, arbitrarily small variance of $\bar{y}$ is theoretically achievable.

4.6.2 PLC-2: Bandwidth Constraint

In deriving PLC-1, the entire class of internally-stabilizing controllers was considered. In this subsection, a PLC is derived based on consideration of only those internally-stabilizing controllers that meet a prespecified bandwidth constraint. Specifically we wish to capture mathematically the notion that no control effort is desired above some frequency, Ω. A convenient method of doing this is to require $S(j\omega) = 1$ to hold for all $\omega > \Omega$. (Strictly speaking, this constraint never

holds exactly, except for the case $C=0$; it's possible to loosen the requirement by allowing $|S(j\omega)-1|$ to be small, but nonzero, for $\omega>\Omega$, but this complicates the notation significantly, and the final conclusions are essentially the same. For the bandwidths quoted in this paper, a 0.05 dB error is permitted in the magnitude plot of S. Using this definition, the bandwidth using C_1 is 7.0 rad/s.) Under such a bandwidth constraint, the following bound holds:

THEOREM 4.2 *For every internally-stabilizing controller whose corresponding sensitivity function satisfies* $S(j\omega)=1$ *for all* $\omega>\Omega$, *the variance of* $\ddot{h}$ *satisfies, for every* $\omega_b>0$,

$$\text{var}(\ddot{h}) = V(K\bar{G})(\omega_b) > \frac{\alpha_1}{\pi}\exp(\alpha_2) + \frac{1}{\pi}\int_{\Omega}^{\infty} |\bar{F}(j\omega)|^2 \, d\omega, \qquad (10)$$

where $\alpha_1 = 2\tan^{-1}(\Omega/z)$ *and* $\alpha_2 = \{\int_0^{\Omega} W(\omega)\ln[|\bar{F}(j\omega)|^2/W(\omega)]\,d\omega\}/\alpha_1$, *and where* $W(\omega)$ *is the weighting function* $2z/(z^2+\omega^2)$.

Figure 10 shows plots of the PLC (10) (hereafter referred to as PLC-2) for several values of Ω; for comparison, PLC-1 is also shown in the figure as a dashed curve. (For each ω_b, α_2 was computed numerically to within 0.1% relative error.) The figure reveals that only the PLC-2 curves with Ω equal to 25 rad/s or larger lie beneath the $0.15g$ threshold for all ω_b in [0.27, 2.7]. In other words, the system bandwidth must be at least 25 rad/s to attain the desired robustness – a considerable increase over the 7.0 rad/s bandwidth of C_1. Moreover, the 25 rad/s figure does not consider the desire for reasonable stability robustness and altitude-holding ability, so it may be necessary to increase the bandwidth even further to satisfy these additional constraints. The next subsection shows that this is indeed the case.

4.6.3 PLC-3: Bandwidth, Stability Robustness, and Holding-Ability Constraints

Suppose that, in addition to the bandwidth constraint imposed for PLC-2, constraints are placed on the stability robustness and on the holding ability of the autopilot. Specifically, suppose it is required that

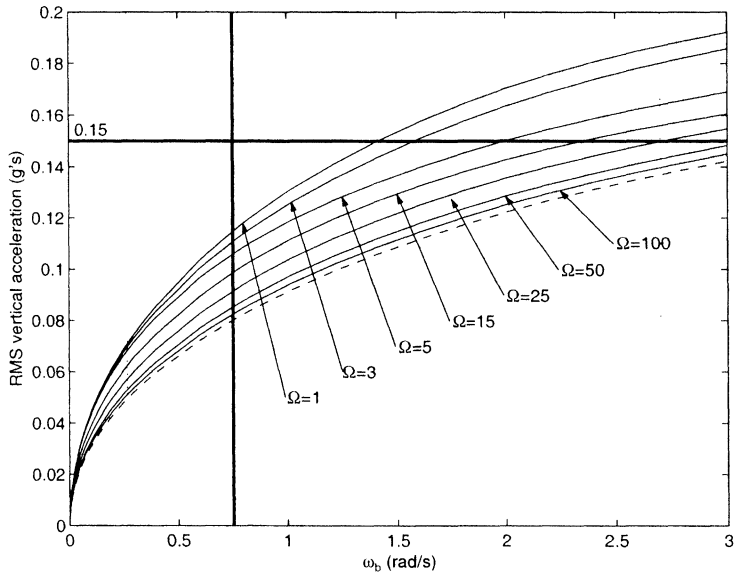

FIGURE 10 Performance limitation curve PLC-2 for several Ω values (all in rad/s), and, for comparison, PLC-1 (dashed). Also included in thick solid lines are the performance threshold and the nominal ω_b value. The two dotted vertical lines mark the ω_b interval of interest.

the stability robustness and holding-ability cannot be worse than those of C_1. This places a total of three constraints on S:

- To ensure that the closed-loop bandwidth is reasonable, require $S(j\omega) = 1$ for $\omega > \Omega$ rad/s;
- To ensure that the distance between the Nyquist plot and the critical point is at least that of C_1, require $\|S\|_\infty < 3.5$ dB; and
- To ensure that the low-frequency altitude tracking is no worse than that of C_1, require $|S(j\omega)| < -30$ dB for $\omega < 0.093$ rad/s.

These three constraints on S are shown as a thick solid boundary in Fig. 5 (for the particular case $\Omega = 7$ rad/s). For general Ω, denote this boundary curve (when not expressed in dB) by $M_{\max}(\omega, \Omega)$. Then the following bound holds:

THEOREM 4.3 *For every internally-stabilizing controller whose corresponding sensitivity function satisfies the above three constraints,*

the variance of $\ddot{h}$ *satisfies, for every* $\omega_b > 0$,

$$\operatorname{var}(\ddot{h}) = V(K\bar{G})(\omega_b) > \frac{1}{\pi}\int_0^{\Omega} \min(M_{\max}^2(\omega,\Omega)|\bar{F}(j\omega)|^2, W(\omega)c^2)\,\mathrm{d}\omega + \frac{1}{\pi}\int_{\Omega}^{\infty} |\bar{F}(j\omega)|^2\,\mathrm{d}\omega, \tag{11}$$

where $W(\omega)$ *is the weighting function* $2z/(z^2+\omega^2)$ *and* c *is the unique scalar satisfying*

$$\int_0^{\Omega} W(\omega)\cdot \ln\left\{\min\left(M_{\max}(\omega,\Omega), \frac{[W(\omega)]^{1/2}c}{|\bar{F}(j\omega)|}\right)\right\}\mathrm{d}\omega = 0. \tag{12}$$

Figure 11 shows plots of the PLC (11) (hereafter referred to as PLC-3) for several values of Ω. (The integration was performed

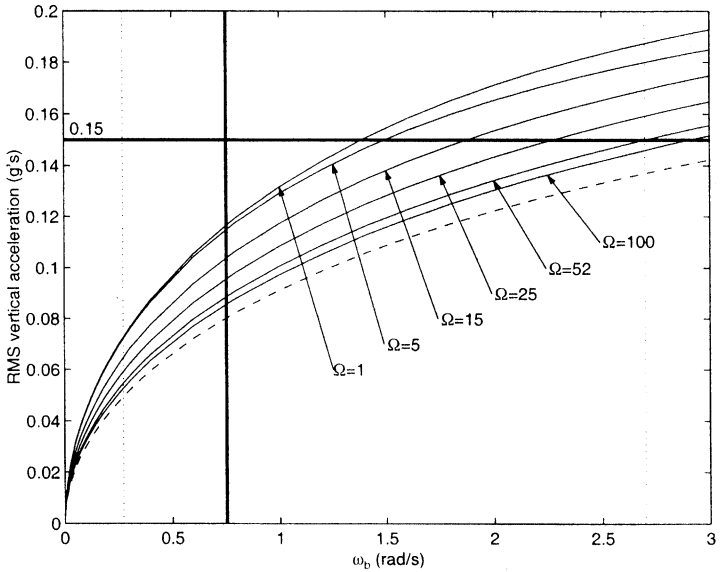

FIGURE 11 Performance limitation curve PLC-3 for several Ω values (all in rad/s), and, for comparison, PLC-1 (dashed). Also included in thick solid lines are the performance threshold and the nominal ω_b value. The two dotted vertical lines mark the ω_b interval of interest.

numerically, as in the PLC-2 case, to within 0.1% relative error. For each ω_b and Ω, constant c in (12) was computed iteratively, to within 0.1% relative error, using the bisection algorithm.) Now only the curves with Ω equal to 52 rad/s or larger lie beneath the $0.15g$ threshold for all ω_b in [0.27, 2.7]. Thus, the system bandwidth must be at least 52 rad/s to attain the desired robustness. This is a significant increase over the 25 rad/s bandwidth that resulted from the PLC-2 analysis, and even more significant compared to the 7.0 rad/s bandwidth of C_1.

Remark 4.2 The performance limitation curves PLC-2 and PLC-3 are based on the Poisson integral that holds due to the plant non-minimum-phase zero (see the Appendix). The Bode sensitivity integral [50] also holds for the plant considered here, and it's not dependent on the non-minimum-phase nature of the plant; using the Bode sensitivity integral instead of the Poisson integral gives different, but very similar, results.

4.7 A Modified Controller

Although this paper deals with analysis, it was felt that at least one alternative controller to C_1 should be presented. Using loop-shaping methods, C_1 was augmented with dynamics in an attempt to increase its robustness. After iterating by trial-and-error, the following controller was arrived at:

$$C_2(s) = -0.0023\frac{(s+0.15)(s+1)^2(s^2+4.2087s+18.26546)/18.26546}{(0.02s+1)(0.35s+1)(0.7s+1)(s^2+72s+1600)/1600}. \tag{13}$$

The dashed curves in Figs. 3–9 correspond to this controller, as do the second rows in Tables II and III. Note that the stability margins (gain margin = 3.46 = 10.8 dB, phase margin = 111 deg, $\|S\|_\infty = 1.43 =$ 3.1 dB) and low-frequency behavior of C_2 (see Figs. 3–5) are essentially the same as those of C_1, but the DBM margin for $\ddot{h}$ has improved significantly (from 1.23 to 2.36). As anticipated, this robustness improvement (which still does not meet the desired robustness) is obtained at a cost of an increase in bandwidth: The gain crossover frequency has increased from 1.0 rad/s to 2.5 rad/s, and control effort

is required up to 400 rad/s, from 7.0 rad/s. The increase in bandwidth is also reflected in the rms ($\dot{u}$) plot (Fig. 9); indeed, DBM for $\dot{u}$ is now below the desired value. It may very well be that this very large increase in bandwidth is unacceptable (due to actuator limitations or unmodeled aircraft dynamics, for example); nevertheless, it follows from the previous section that, if significant improvement in the robustness is desired, there is simply no choice but to increase the bandwidth.

5 CONCLUSIONS

The notions of V-transform, disturbance bandwidth margin, and disturbance gain margin were introduced to analyze uncertainty in disturbance bandwidth and gain. They were used to analyze the behavior of an altitude-hold autopilot system in the face of uncertain turbulence characteristics. In particular, it was shown that the autopilot achieves good nominal performance, as measured by the variance of several signals; however, when uncertainty in the turbulence bandwidth is considered, the autopilot performance is inadequate as measured by the variance of the vertical acceleration. Several performance limitation curves were then derived to determine a lower bound on how much the system bandwidth must be increased to attain the desired robustness. It was concluded that, if one is willing to sacrifice stability robustness and altitude-holding ability, the controller bandwidth must be increased from 7.0 rad/s to at least 25 rad/s; if such a sacrifice cannot be made, then the bandwidth must be increased even further, to at least 52 rad/s. With regard to future research, it is desirable to extent the results from analysis to design; some progress along this line is reported in [51].

Acknowledgments

This research was supported by the Army Research Office under Grant DAAL03-92-G-0127. The first author would also like to acknowledge funding from the Natural Sciences and Engineering Research Council of Canada. Finally, we thank Munir Orgun and Earl Weener of the Boeing Company for their interest in, and feedback on, this work.

APPENDIX

Proof of Theorem 2.1 Equation (3) is derived first. On noting that $F(s) = (2\omega_b)^{1/2}/(s+\omega_b) = \left[\begin{array}{c|c} -\omega_b & (2\omega_b)^{1/2} \\ \hline 1 & 0 \end{array}\right](s)$, it follows that

$$\bar{G}(s)\cdot F(s) = \left[\begin{array}{c|c} A & B \\ \hline C & D \end{array}\right](s)\cdot\left[\begin{array}{c|c} -\omega_b & (2\omega_b)^{1/2} \\ \hline 1 & 0 \end{array}\right](s)$$

$$= \left[\begin{array}{cc|c} A & B & 0 \\ 0 & -\omega_b & (2\omega_b)^{1/2} \\ \hline C & D & 0 \end{array}\right](s). \tag{14}$$

Let L denote the observability Grammian of this realization of $\bar{G}F$. Partition L as

$$L = \begin{bmatrix} L_1 & L_2^{\mathrm{T}} \\ L_2 & L_3 \end{bmatrix},$$

where L_3 is a scalar. Then,

$$V(\bar{G})(\omega_b) = \|\bar{G}F\|_2^2 = \begin{bmatrix} 0 & (2\omega_b)^{1/2} \end{bmatrix} L \begin{bmatrix} 0 \\ (2\omega_b)^{1/2} \end{bmatrix} = 2\omega_b L_3. \tag{15}$$

We now solve for L_3 for substitution in 15. The Lyapunov equation for the observability Grammian of $\left([C \quad D], \begin{bmatrix} A & B \\ 0 & -\omega_b \end{bmatrix}\right)$ is

$$\begin{bmatrix} A & B \\ 0 & -\omega_b \end{bmatrix}^{\mathrm{T}} \begin{bmatrix} L_1 & L_2^{\mathrm{T}} \\ L_2 & L_3 \end{bmatrix} + \begin{bmatrix} L_1 & L_2^{\mathrm{T}} \\ L_2 & L_3 \end{bmatrix} \begin{bmatrix} A & B \\ 0 & -\omega_b \end{bmatrix}$$

$$+ [C \quad D]^{\mathrm{T}} [C \quad D] = 0.$$

This matrix equation is equivalent to the following three equations:

$$A^{\mathrm{T}}L_1 + L_1 A + C^{\mathrm{T}}C = 0, \tag{16}$$

$$B^{\mathrm{T}}L_1 - \omega_b L_2 + L_2 A + DC = 0, \tag{17}$$

$$B^{\mathrm{T}}L_2^{\mathrm{T}} - \omega_b L_3 + L_2 B - \omega_b L_3 + D^2 = 0. \tag{18}$$

Equation (16) indicates that L_1 is the observability Grammian of (C, A); denote this Grammian by L_o. By the stability of $\bar{G}$, ω_b is not an eigenvalue of A; hence, $(A-\omega_b I)^{-1}$ exists, and solving for L_2 in (17) yields

$$L_2 = (-B^{\mathrm{T}} L_o - DC)(A - \omega_b I)^{-1}. \tag{19}$$

Next, solve for scalar L_3 in (18) and substitute for L_2 using (19) to obtain

$$L_3 = \frac{1}{2\omega_b} D^2 - \frac{1}{\omega_b}(B^{\mathrm{T}} L_o - DC)(A - \omega_b I)^{-1} B.$$

Use this to substitute for L_3 in (15):

$$V(\bar{G})(\omega_b) = D^2 + 2(B^{\mathrm{T}} L_o + DC)(\omega_b I - A)^{-1} B,$$

which proves the result.

The second point in the theorem is simple: $V(\bar{G})(\omega_b)$ is nonnegative since it is a norm; $V(\bar{G})$ is an analytic function of ω_b since it is a rational function of ω_b with all poles in the open left half-plane; $V(\bar{G})$ is a bounded function of ω_b since it is a *proper* rational function of ω_b with all poles in the open left half-plane. To prove the third point in the theorem, write

$$V(\bar{G})(\omega_b) = \frac{1}{\pi}\int_0^\infty |\bar{G}(j\omega)|^2 \frac{2\omega_b}{\omega^2 + \omega_b^2}\,\mathrm{d}\omega = \frac{2}{\pi}\int_0^\infty |\bar{G}(j\omega_b\alpha)|^2 \frac{1}{\alpha^2+1}\,\mathrm{d}\alpha$$

and compute the limit

$$\begin{aligned}
\lim_{\omega_b \to 0} V(\bar{G})(\omega_b) &= \lim_{\omega_b \to 0} \frac{2}{\pi}\int_0^\infty |\bar{G}(j\omega_b\alpha)|^2 \frac{1}{\alpha^2+1}\,\mathrm{d}\alpha \\
&= \frac{2}{\pi}\int_0^\infty \lim_{\omega_b \to 0} |\bar{G}(j\omega_b\alpha)|^2 \frac{1}{\alpha^2+1}\,\mathrm{d}\alpha \\
&= \frac{2\bar{G}(0)^2}{\pi}\int_0^\infty \frac{1}{\alpha^2+1}\,\mathrm{d}\alpha \\
&= \bar{G}(0)^2.
\end{aligned}$$

(For rigorous justification of taking the limit under the integral sign, apply Theorem 17.3c in [52].) The fourth point in the theorem follows immediately from realization (3).

Proof of Theorem 4.1 The bound is obtained by constructing the minimum-variance controller. The construction closely follows the procedure described in Section 10.4 of [53], so the derivation is condensed.

The first step is to compute a coprime factorization for P_1P_2, that is, compute stable proper transfer functions N, M, X, and Y so that (the Laplace variable is omitted for brevity):

$$P_2P_1 = \frac{N}{M} \quad \text{and} \quad NX + MY = 1.$$

(See [53] for methods of computing N, M, X, and Y.) Then it's a standard result that the set of internally-stabilizing controllers is parameterized by the so-called Youla parameter Q (a stable transfer function). In particular, the set is

$$\left\{ \frac{X + MQ}{Y - NQ} : Q \text{ is stable} \right\}.$$

It's now a matter of finding the Q that minimizes the output variance. To this end, define the stable transfer functions

$$T = HP_2FMN \quad \text{and} \quad Z = HP_2FMY.$$

Let T_{ap} denote the all-pass component of T and T_{mp} the minimum-phase component of T so that $T = T_{\text{ap}}T_{\text{mp}}$. Then it's straightforward to show that

$$V(G)(\omega_b) = \|GF\|_2^2 = \|Z - TQ\|_2^2 = \|T_{\text{ap}}^{-1}Z - T_{\text{mp}}Q\|_2^2. \tag{20}$$

The next step is to decompose $T_{\text{ap}}^{-1}Z$ into stable and completely unstable (all poles in the open right-half-plane) parts:

$$T_{\text{ap}}^{-1}Z = (T_{\text{ap}}^{-1}Z)_{\text{st}} + (T_{\text{ap}}^{-1}Z)_{\text{un}}.$$

Substitute this into (20) and use a version of the Pythagoras theorem (see [53]) to obtain

$$V(G)(\omega_b) = \|(T_{\text{ap}}^{-1}Z)_{\text{un}}\|_2^2 + \|(T_{\text{ap}}^{-1}Z)_{\text{st}} - T_{\text{mp}}Q\|_2^2. \tag{21}$$

From this equation, it is apparent that the minimum value of $V(G)(\omega_b)$ is (as a function of ω_b)

$$\|(T_{ap}^{-1}Z)_{un}\|_2^2.$$

Computation and substitution of M, N, X, and Y (and multiplication by K^2) yields (8). The tightness of the bound also follows from (21): The second term in (21) is zero at $Q = T_{mp}^{-1}(T_{ap}^{-1}Z)_{st}$. (Since this Q is improper, it must be approximated by a proper transfer function. Another technicality overlooked is that this optimal Q will have a pole at the origin, and, therefore, the closed-loop system will be unstable; this can be overcome by shifting the pole at the origin of P_2 and the zeros at the origin of H slightly into the left-hand plane.)

Proof of Theorem 4.2 The idea behind the proof is to treat the function $|S(j\omega)|$ as a curve in $\omega \in [0, \Omega]$, and apply classical optimal control theory to find the curve that minimizes the variance of $\bar{y}$. The optimization is carried out subject to the constraint

$$\int_0^\infty \ln|S(j\omega)|W(\omega)\,d\omega = 0, \tag{22}$$

where $W(\omega) = 2z/(z^2+\omega^2)$. This constraint, usually called a "Poisson integral" constraint, arises because of the non-minimum-phase zero at $s = z$. See [50] for the general Poisson integral derivation.

For convenience, define the functions $f(\omega) = \ln|S(j\omega)|^2$ and $g(\omega) = \ln|\bar{F}(j\omega)|^2$. Use (22) and the assumption that $|S(j\omega)| = 1$ for $\omega > \Omega$ to obtain

$$\int_0^\Omega f(\omega)W(\omega)\,d\omega = 0. \tag{23}$$

Now compute the variance of $\bar{y}$:

$$\begin{aligned}
\text{var}(\bar{y}) &= \frac{1}{\pi}\int_0^\infty |\bar{F}(j\omega)|^2|S(j\omega)|^2\,d\omega \\
&= \frac{1}{\pi}\int_0^\Omega |\bar{F}(j\omega)|^2|S(j\omega)|^2\,d\omega + \frac{1}{\pi}\int_\Omega^\infty |\bar{F}(j\omega)|^2\,d\omega \\
&= \frac{1}{\pi}\int_0^\Omega \exp(g(\omega)+f(\omega))\,d\omega + \frac{1}{\pi}\int_\Omega^\infty |\bar{F}(j\omega)|^2\,d\omega. \qquad (24)
\end{aligned}$$

Thus, the optimization problem reduces to finding the f that minimizes

$$\int_0^{\Omega} \exp(g(\omega) + f(\omega))\, d\omega$$

subject to (23). To rewrite this in a more convenient form, define, for $\omega \in [0, \Omega]$,

$$h(\omega) = \int_0^{\omega} f(\bar{\omega}) W(\bar{\omega})\, d\bar{\omega}.$$

Then the problem reduces to the following subproblem:

$$\min_f \int_0^{\Omega} L(h, f, \omega)\, d\omega \tag{25}$$

$$\text{where} \quad L(h, f, \omega) = \exp(f(\omega) + g(\omega)) \tag{26}$$

$$\text{subject to} \quad \dot{h}(\omega) = f(\omega) W(\omega) \tag{27}$$

$$\text{with end conditions} \quad h(0) = 0, \quad h(\Omega) = 0. \tag{28}$$

This subproblem has been written as a control problem where f plays the role of the control signal and h plays the role of the state. The "dot" notation denotes differentiation with respect to ω.

The solution of (25)–(28) can be found by applying classical unconstrained optimal control theory [54]. The Hamiltonian is

$$H(h, f, \omega) = L(h, f, \omega) + \lambda f W = \exp(f + g) + \lambda f W,$$

where λ is the costate, i.e., the solution to $-\dot{\lambda} = \partial H / \partial h$. Since $\partial H / \partial h = 0$, it follows that λ is constant. Next, the stationarity condition $\partial H / \partial f = 0$ yields

$$\exp(f + g) + \lambda W = 0.$$

Since W is positive, this implies that λ is negative and that the optimal "control signal" is

$$f(\omega) = \ln W(\omega) - g(\omega) + c_1,$$

where $c_1 \triangleq \ln(-\lambda)$. To evaluate c_1, use $\dot{h} = fW$ to obtain

$$\dot{h}(\omega) = [\ln W(\omega) - g(\omega) + c_1]W(\omega).$$

Integration yields

$$h(\omega) = \int_0^\omega W(\bar{\omega})[\ln W(\bar{\omega}) - g(\bar{\omega})]\,\mathrm{d}\bar{\omega} + c_1 \int_0^\omega W(\bar{\omega})\,\mathrm{d}\bar{\omega} + c_0,$$

where c_o is a second constant. Using the constraints $h(0) = 0$ and $h(\Omega) = 0$ uniquely determines c_0 and c_1 to be

$$c_0 = 0 \text{ and } c_1 = \frac{\int_0^\Omega W(\bar{\omega})[g(\bar{\omega}) - \ln W(\bar{\omega})]\,\mathrm{d}\bar{\omega}}{\int_0^\Omega W(\bar{\omega})\,\mathrm{d}\bar{\omega}}.$$

Therefore, the optimal f is

$$f(\omega) = \ln W(\omega) - g(\omega) + \frac{\int_0^\Omega W(\bar{\omega})[g(\bar{\omega}) - \ln W(\bar{\omega})]\,\mathrm{d}\bar{\omega}}{\int_0^\Omega W(\bar{\omega})\,\mathrm{d}\bar{\omega}},$$

and the optimal cost is

$$\int_0^\Omega \exp(f(\omega) + g(\omega))\,\mathrm{d}\omega$$
$$= \int_0^\Omega W(\omega)\,\mathrm{d}\omega \cdot \exp\left\{\frac{\int_0^\Omega W(\omega)[g(\omega) - \ln W(\omega)]\,\mathrm{d}\omega}{\int_0^\Omega W(\omega)\,\mathrm{d}\omega}\right\}. \quad (29)$$

This solves the subproblem (25)–(28). Substitution of (29) into (24) yields

$$\mathrm{var}(\bar{y}) \geq \frac{1}{\pi}\int_0^\Omega W(\omega)\,\mathrm{d}\omega \cdot \exp\left\{\frac{\int_0^\Omega W(\omega)[\ln|\bar{F}(j\omega)|^2 - \ln W(\omega)]\,\mathrm{d}\omega}{\int_0^\Omega W(\omega)\,\mathrm{d}\omega}\right\}$$
$$+ \frac{1}{\pi}\int_\Omega^\infty |\bar{F}(j\omega)|^2\,\mathrm{d}\omega.$$

Bound (10) follows immediately on defining $\alpha_1 = \int_0^\Omega W(\omega)\,\mathrm{d}\omega = 2\tan^{-1}\Omega/z$ and $\alpha_2 = \{\int_0^\Omega W(\omega)\ln[|\bar{F}(j\omega)|^2/W(\omega)]\,\mathrm{d}\omega\}/\alpha_1$.

Proof of Theorem 4.3 The key idea, as in the proof of Theorem 4.2, is to treat the function $|S(j\omega)|$ as a curve in $\omega \in [0, \Omega]$, and apply classical optimization theory to find the curve that minimizes the variance of $\bar{y}$. The optimization is carried out subject to the Poisson integral constraint given in (22) and subject to the constraint $|S(j\omega)| \leq M_{\max}(\omega, \Omega)$. The addition of the second constraint, absent in the previous proof, mandates the use of more sophisticated mathematical tools.

As in the proof of Theorem 4.2, define the functions $f(\omega) = \ln|S(j\omega)|^2$ and $g(\omega) = \ln|\bar{F}(j\omega)|^2$. Also define $M(\omega) = \ln M_{\max}^2(\omega, \Omega)$. (The dependence on parameter Ω is not explicitly shown.) Use (22) and the assumption that $|S(j\omega)| = 1$ for $\omega > \Omega$ to obtain, exactly as before (see (24)):

$$\operatorname{var}(\bar{y}) = \frac{1}{\pi}\int_0^{\Omega} \exp(g(\omega) + f(\omega))\, d\omega + \frac{1}{\pi}\int_{\Omega}^{\infty} |\bar{F}(j\omega)|^2\, d\omega. \tag{30}$$

Thus, the optimization problem reduces to finding the f that minimizes

$$\int_0^{\Omega} \exp(g(\omega) + f(\omega))\, d\omega$$

subject to (23) and subject to $f(\omega) \leq M(\omega)$. This problem can be converted into a standard form for application of Pontryagin's Minimum Principle (see [54]). To this end, define, for $\omega \in [0, \Omega]$,

$$h(\omega) = \int_0^{\omega} f(\bar{\omega}) W(\bar{\omega})\, d\bar{\omega}.$$

Then the problem reduces to the following subproblem:

$$\min_f \int_0^{\Omega} L(h, f, \omega)\, d\omega \tag{31}$$

$$\text{where} \quad L(h, f, \omega) = \exp(f(\omega) + g(\omega)) \tag{32}$$

$$\text{subject to} \quad \dot{h}(\omega) = f(\omega) W(\omega) \tag{33}$$

$$\text{with end conditions} \quad h(0) = 0, \quad h(\Omega) = 0 \tag{34}$$

$$\text{and control constraint} \quad f(\omega) \leq M(\omega). \tag{35}$$

As before, this is an optimization problem where f plays the role of the control signal and h plays the role of the state. The Hamiltonian is

$$H(h,f,\omega) = L(h,f,\omega) + \lambda f W = \exp(f+g) + \lambda f W,$$

where λ is the costate, i.e., the solution to $-\dot{\lambda} = \partial H/\partial h$. Since $\partial H/\partial h = 0$, it follows that λ is constant. Pontryagin's Minimum Principle states that the optimal control, $f(\omega)$, is that which minimizes the Hamiltonian (when evaluated at the optimal state and costate) over all admissible controls. Here, this means that the optimal control is the $f(\omega)$ that minimizes

$$\exp(f(\omega) + g(\omega)) + \lambda f(\omega) W(\omega), \tag{36}$$

where λ is the optimal costate (yet to be determined) and where $f(\omega)$ is constrained by $f(\omega) \leq M(\omega)$. This holds at each $\omega \in [0, \Omega]$. There are two cases:

- If $\lambda \geq 0$, then function (36) is clearly "minimized" at $f(\omega) = -\infty$. Since λ is a constant, this implies that $f(\omega) = -\infty$ for all $\omega \in [0, \Omega]$. However, such a control signal does not satisfy $\int_0^\Omega f(\omega) W(\omega)\, d\omega = 0$, so this case cannot occur.
- If $\lambda < 0$, then simple analysis shows that (36), as a function of $f(\omega)$, has exactly one stationary point (a global minimum) at $f(\omega) = \ln(-\lambda W(\omega)) - g(\omega)$. Therefore, the optimal control, in terms of the still unknown λ, is

$$\begin{aligned} f(\omega) &= \min(M(\omega), \ln(-\lambda W(\omega)) - g(\omega)) \\ &= \min(M(\omega), \ln W(\omega) - g(\omega) + c_1), \end{aligned} \tag{37}$$

where $c_1 \triangleq \ln(-\lambda)$. We can solve for c_1 by applying the constraint

$$\int_0^\Omega f(\omega) W(\omega)\, d\omega = 0. \tag{38}$$

This yields

$$\int_0^\Omega W(\omega) \cdot \min(M(\omega), \ln W(\omega) - g(\omega) + c_1)\, d\omega = 0. \tag{39}$$

Equation (39) can be solved for c_1 via the bisection algorithm since the right-hand side is a known quantity and the left-hand side is a monotonically increasing function of c_1. (A solution exists if and only if $\int_0^\Omega W(\omega)M(\omega)\,\mathrm{d}\omega \geq 0$, which holds here for sufficiently large Ω.) The optimal cost is

$$\begin{aligned}
&\int_0^\Omega \exp\{f(\omega)+g(\omega)\}\,\mathrm{d}\omega \\
&\quad = \int_0^\Omega \exp\{\min(M(\omega),\, \ln W(\omega) - g(\omega) + c_1) + g(\omega)\}\,\mathrm{d}\omega \\
&\quad = \int_0^\Omega \exp\{\min(M(\omega)+g(\omega),\, \ln W(\omega) + c_1)\}\,\mathrm{d}\omega. \qquad (40)
\end{aligned}$$

This solves the subproblem (31)–(35). Substitution of (40) into (30) yields, after simple manipulation,

$$\begin{aligned}
\mathrm{var}(\bar{y}) \geq \frac{1}{\pi}\int_0^\Omega \min(M_{\max}^2(\omega,\Omega)|\bar{F}(j\omega)|^2,\, W(\omega)\exp(c_1))\,\mathrm{d}\omega \\
+ \frac{1}{\pi}\int_\Omega^\infty |\bar{F}(j\omega)|^2\,\mathrm{d}\omega.
\end{aligned}$$

Define $c \triangleq \exp(c_1/2)$ to obtain (11). The equation for c follows from (39).

References

[1] National Transportation Safety Board, "Incident identification IAD99FA052," Washington, DC, 20594, 1999. (also see http://www.ntsb.gov/Aviation/AD/99A052.htm).

[2] B. Etkin, "Turbulent wind and its effect on flight," *AIAA Journal of Aircraft*, **18**, 327–345, May 1981.

[3] B. Etkin and L.D. Reid, *Dynamics of Flight: Stability and Control*, Chap. 8, John Wiley & Sons, New York, 3rd edn., 1996.

[4] J. Roskam, *Airplane Flight Dynamics and Automatic Flight Controls: Part II*, Chap. 9, Roskam Aviation and Engineering Corporation, Kansas City, 1979.

[5] J. Roskam, *Airplane Design Part VII: Determination of Stability, Control and Performance Characterstitics – FAR and Military Requirements*, Chap. 4 & App. B, Roskam Aviation and Engineering Corporation, Route 4, Box 274, Ottawa, Kansas, 66067, 1985.

[6] C. Dodds and J. Robson, "The description of road surface roughness," *Journal of Sound and Vibration*, **31**, 175–183, November 1973.

[7] A. Hać, "Adaptive control of vehicle suspension," *Vehicle System Dynamics*, **16**(2), 57–74, 1987.

[8] A. Healey, E. Nathman and C. Smith, "An analytical and experimental study of automobile dynamics with random roadway inputs," *Transactions of the ASME: Journal of Dynamic Systems, Measurement, and Control*, **99**, 284–292, December 1977.

[9] D. Hrovat, "Applications of optimal control to advanced automotive suspension design," *Transactions of the ASME: Journal of Dynamic Systems, Measurement, and Control*, **115**, 328–342, June 1993.

[10] X.-P. Lu, "Effects of road roughness on vehicular rolling resistance," in *Measuring Road Roughness and Its Effects on User Cost and Comfort* (T.D. Gillespie and M. Sayers, Eds.), (Philadelphia), pp. 143–161, ASTM, 1985.

[11] R. Bishop and W. Price, *Hydroelasticity of Ships*, Chap. 11, Cambridge University Press, London, 1979.

[12] J.B. Herbich (Ed.), *Handbook of Coastal and Ocean Engineering*, Vol. 1, Chap. 7, Gulf Publishing, Houston, Texas, 1990.

[13] A. Lloyd, *Seakeeping: Ship Behaviour in Rough Weather*, Chap. 4, John Wiley & Sons, New York, 1989.

[14] J.R. Elliott, "NASA's advanced control law program for the F-8 digital fly-by-wire aircraft," *IEEE Transactions on Automatic Control*, **AC-22**(5), 753–757, 1977.

[15] D.E. Davison, P.T. Kabamba and S.M. Meerkov, "Limitations of disturbance rejection in feedback systems with finite bandwidth," *IEEE Transactions on Automatic Control*, **44**(6), 1132–1144, 1999.

[16] C. Gökçek, D.E. Davison, P.T. Kabamba and S.M. Meerkov, "Robustness of control systems with respect to disturbance model uncertainty," in *14th IFAC World Congress*, Vol. G, (Beijing), pp. 289–294, IFAC, 1999.

[17] W.R. Hudson, D. Halbach, J.P. Zaniewski and L. Moser, "Root-mean-square vertical acceleration as a summary roughness statistic," in *Measuring Road Roughness and its Effects on User Cost and Comfort* (T.D. Gillespie and M. Sayers, Eds.), (Philadelphia), pp. 3–24, ASTM, 1985.

[18] C. Smith, D. McGehee and A. Healey, "The prediction of passenger riding comfort from acceleration data," *Transactions of the ASME: Journal of Dynamic Systems, Measurement, and Control*, **100**, 34–41, March 1978.

[19] S. Kim, S.M. Meerkov and T. Runolfsson, "Aiming control: Design of residence probability controllers," *Automatica*, **28**(3), 557–564, 1992.

[20] S. Kim, S.M. Meerkov and T. Runolfsson, "Aiming control: Residence probability and (d, t)-stability," *Automatica*, **28**(3), 549–555, 1992.

[21] S.M. Meerkov and T. Runolfsson, "Output residence time control," *IEEE Transactions on Automatic Control*, **34**(11), 1171–1176, 1989.

[22] F.M. Hoblit, *Gust Loads on Aircraft: Concepts and Applications*, Chap. 4, AIAA Education Series, American Institute of Aeronautics and Astronautics, Washington, DC, 1988. (originally published as a Lockheed Report).

[23] D. McRuer, I. Ashkenas and D. Graham, *Aircraft Dynamics and Automatic Control*, Princeton University Press, Princeton, New Jersey, 1973.

[24] W. Price and R. Bishop, *Probabilistic Theory of Ship Dynamics*, Chap. 9, John Wiley & Sons, New York, 1974.

[25] R. Skelton and M. Ikeda, "Covariance controllers for linear continuous-time systems," *International Journal of Control*, **49**(5), 1773–1785, 1989.

[26] V. Poor and D.P. Looze, "Minimax state estimation for linear stochastic systems with noise uncertainty," *IEEE Transactions on Automatic Control*, **AC-26**, 902–906, August 1981.

[27] S.A. Kassam and T.L. Lim, "Robust Wiener filters," *Journal of the Franklin Institute*, **304**, 171–185, 1977.

[28] G. Moustakides and S.A. Kassam, "Robust Wiener filters for random signals in correlated noise," *IEEE Transactions on Information Theory*, **IT-29**, 614–619, July 1983.

[29] S.A. Kassam and T.L. Lim and L.J. Cimini, "Two-dimensional filters for signal processing under modeling uncertainties," *IEEE Transactions on Geoscience and Remote Sensing*, **GE-18**, 331–336, October 1980.
[30] H.V. Poor, "On robust Wiener filtering," *IEEE Transactions on Automatic Control*, **AC-25**, 531–536, June 1980.
[31] D.P. Looze, H.V. Poor, K.S. Vastola and J.C. Darragh, "Minimax control of linear stochastic systems with noise uncertainty," *IEEE Transactions on Automatic Control*, **AC-28**, 882–888, September 1983.
[32] B.-S. Chen and T.-Y. Dong, "LQG optimal control system design under plant perturbation and noise uncertainty: A state-space approach," *Automatica*, **25**(3), 431–436, 1989.
[33] S.-H. Chen, J.-H. Chou and C.-H. Chao, "Stability robustness of the LQG system with noise uncertainty and nonlinear/linear time-varying plant perturbations," *JSME International Journal, Series C*, **39**, 67–72, March 1996.
[34] J.S. Luo and A. Johnson, "Stability robustness of the continuous-time LQG system under plant perturbation and noise uncertainty," *Automatica*, **29**(2), 485–489, 1993.
[35] S.V. Gusev, "Minimax control under a bound on the partial covariance sequence of the disturbance," *Automatica*, **31**(9), 1287–1301, 1995.
[36] S.V. Gusev, "Minimax control under a restriction of the moments of disturbance," in *Proceedings of 34th Conference on Decision and Control*, (New Orleans, LA), pp. 1195–1200, IEEE, December 1995.
[37] S.V. Gusev, "Method of moment restrictions in robust control and filtering," in *IFAC World Congress*, (San Francisco), pp. 415–420, IFAC, July 1996.
[38] T. Greenlee and C.T. Leondes, "Generalized bounding filters for linear time invariant systems," in *Decision and Control Conference*, (New Orleans, LA), pp. 585–590, IEEE, December 1977.
[39] N.E. Nahi and I.M. Weiss, "Optimum Wiener bounding filters in the presence of uncertainties," *Information and Control*, **28**, 179–191, July 1975.
[40] N.E. Nahi and I.M. Weiss, "Bounding filter: A simple solution to loack of exact *a priori* statistics," *Information and Control*, **39**, 212–224, November 1978.
[41] V.A. Yakubovich, "Optimal damping of forced stochastic oscillations in linear systems in the case of unknown spectral density of external disturbance," in *Proceedings of the 35th Conference on Decision and Control*, (Kobe, Japan), pp. 3200–3203, IEEE, December 1996.
[42] M.J. Grimble, "LQG optimal control design for uncertain systems," *IEE Proceedings-D*, **139**, 21–30, January 1992.
[43] L.R. Ray, "Robust linear-optimal control laws for active suspension systems," in *The Winter Annual Meeting of the ASME: Advanced Automotive Technologies 1991*, pp. 291–302, December 1991.
[44] P.H. McDowell and T. Basar, "Robust controller design for linear stochastic systems with uncertain parameters," in *1986 American Control Conference*, Vol. 1, (Seattle, WA), pp. 39–44, IEEE, June 1986.
[45] X.Y. Gu and W.H. Chen, "Design of suboptimal minimax LQG controller via game theory," in *American Control Conference*, Vol. 1, (Boston, MA), pp. 376–377, IEEE, June 1991.
[46] D.S. Bernstein and S.W. Greeley, "Robust controller synthesis using the maximum entropy design equations," *IEEE Transactions on Automatic Control*, **AC-31**, 362–364, April 1986.
[47] M. Tahk and J.L. Speyer, "Modeling of parameter variations and asymptotic LQG synthesis," in *Proceedings of the 25th Conference on Decision and Control*, Vol. 3, (Athens, Greece), pp. 1459–1465, IEEE, December 1986.
[48] M. Tahk and J.L. Speyer, "A parameter robust LQG design synthesis with applications to control of flexible structures," in *1987 American Control Conference*, Vol. 1, (Minneapolis, MN), pp. 386–392, IEEE, June 1987.

[49] D.E. Davison, P.T. Kabamba and S.M. Meerkov, "The V-transform: A tool for robustness analysis with respect to disturbance model uncertainty," *Mathematical Problems in Engineering*, **3**, 413–477, 1997.
[50] J.S. Freudenberg and D.P. Looze, "Right half-plane poles and zeros and design tradeoffs in feedback systems," *IEEE Transactions on Automatic Control*, **AC-30**, 555–565, June 1985.
[51] D.E. Davison, *Robustness of Disturbance Attenuation with Respect to Disturbance Model Uncertainty*. Ph.D. dissertation, University of Michigan, 1997.
[52] W. Fulks, *Advanced Calculus: An Introduction to Analysis*, p. 606, John Wiley and Sons, New York, NY, 3rd edn., 1978.
[53] J.C. Doyle, B.A. Francis and A.R. Tannenbaum, *Feedback Control Theory*, Chap. 5 & 10, Macmillan, New York, NY, 1992.
[54] F.L. Lewis, *Optimal Control*, Chap. 3, John Wiley & Sons, New York, 1986.